

## THERMOPLASTIC WAVES IN MAGNETARS

ANDREI M. BELOBORODOV<sup>1</sup> AND YURI LEVIN<sup>2</sup>

<sup>1</sup>Physics Department and Columbia Astrophysics Laboratory, Columbia University, 538 West 120th Street New York, NY 10027;  
 amb@phys.columbia.edu and

<sup>2</sup> Monash Center for Astrophysics and School of Physics, Monash University, Clayton, VIC 3800, Australia; yuri.levin@monash.edu.au  
*Draft version October 4, 2018*

### ABSTRACT

Magnetar activity is generated by shear motions of the neutron star surface, which relieve internal magnetic stresses. An analogy with earthquakes and faults is problematic, as the crust is permeated by strong magnetic fields, which greatly constrain crustal displacements. We describe a new deformation mechanism that is specific to strongly magnetized neutron stars. The magnetically stressed crust begins to move because of a thermoplastic instability, which launches a wave that shears the crust and burns its magnetic energy. The propagating wave front resembles the deflagration front in combustion physics. We describe the conditions for the instability, the front structure and velocity, and discuss implications for observed magnetar activity.

*Subject headings:* dense matter — instabilities — magnetic fields — waves — stars: magnetars — stars: neutron

### 1. INTRODUCTION

The activity of magnetars is explained by their crustal motions that twist the neutron star magnetosphere (Thompson et al. 2002) and ignite electron-positron discharge (Beloborodov & Thompson 2007). The continual  $e^\pm$  flow around the magnetar generates the observed hard X-ray emission (Beloborodov 2013; An et al. 2013; Hascoët et al. 2013). Magnetospheric twisting also explains the variable spindown rate and may be responsible for triggering flares (Thompson & Duncan 1996; Lyutikov 2006; Parfrey et al. 2013).

Theoretical calculations show that a magnetospheric twist dissipates in a few years, in agreement with the timescale of flux decay in transient magnetars (e.g. Mereghetti 2008) and observations of slowly shrinking hot spots (Gotthelf & Halpern 2007; Beloborodov 2011). The twist injection must occur faster than dissipation, so the twist is created by crustal motions with vorticity  $> 1 \text{ rad yr}^{-1}$ . This is orders of magnitude faster than the accumulation of internal stresses due to ambipolar diffusion or Hall drift (Goldreich & Reisenegger 1992; Thompson & Duncan 1996), and hence a quickly developing instability is involved in the crust yielding to the stresses.

How this instability occurs is an open question. Cracks are impossible because the crust has huge pressure (Jones 2003). Large slips are forbidden by the presence of strong magnetic fields, unless they are aligned within  $10^{-3}$  radian with magnetic flux surfaces (Levin & Lyutikov 2012). One plausible yielding mechanism is a plastic flow. This possibility is especially attractive for the inner crust, which may have an alloy-type lattice (Kobyakov & Pethick 2014).

The internal stresses gradually accumulate over the lifetime of the star (Viganò et al. 2013). They cause elastic crustal deformations until the stress exceeds a critical value  $\sigma_{\text{cr}}$ . A significant plastic motion can be initiated at this point. Its development is assisted by heat generated by the plastic flow. We will show below that this leads to an instability launching a thermo-plastic wave

(TPW) resembling a deflagration front. The propagating wave dissipates the magnetic energy inside the crust and creates the external magnetic twist.

### 2. BASIC EQUATIONS

We will describe the mechanism of TPW using the simplest configuration where the crust is a slab with density  $\rho(z)$  threaded by uniform vertical magnetic field  $B_z$ . The hydrostatic balance between two strong vertical forces (gravity and pressure gradient) constrains possible crustal displacements to the horizontal  $x$ - $y$  plane. The crust is almost incompressible, and therefore  $B_z$  remains constant. The model is effectively one-dimensional: the horizontal components of magnetic field  $B_x$ ,  $B_y$  and displacement  $\xi_x$ ,  $\xi_y$  are functions of  $z$  only. Furthermore, for simplicity we take  $B_x = 0 = \xi_x$ . An axisymmetric generalization will be briefly described in Section 5.

The plastic flow velocity is much smaller than the Alfvén and shear speeds in the crust. Therefore the elastic and magnetic forces are nearly balanced,

$$\frac{\partial}{\partial z} \left( \frac{B_y B_z}{4\pi} - \sigma \right) = 0, \quad (1)$$

where  $\sigma = \sigma_{zy}$  is the shear stress of the crustal lattice. This gives

$$b \mu_B - \sigma = \mu_B b_{\text{ext}}, \quad (2)$$

where

$$\mu_B \equiv \frac{B_z^2}{4\pi}, \quad b \equiv \frac{B_y}{B_z}, \quad (3)$$

and  $b_{\text{ext}}$  describes the magnetic field above the crust. Below, we demonstrate the TPW mechanism with  $b_{\text{ext}} \approx 0$ ; the effect of  $b_{\text{ext}} \neq 0$  is considered in Section 5.

If the crust deformation was purely elastic, its strain  $s = \partial\xi/\partial z$  would be given by

$$s_{\text{el}} = -\frac{\sigma}{\mu}, \quad (4)$$

where  $\mu$  is the lattice shear modulus. When  $\sigma$  exceeds some critical value  $\sigma_{\text{cr}}$ , a plastic shear flow is produced.

This may occur either due to the activation of motion of microscopic lattice defects (e.g. Mason 1960), or due to the nucleation of a multitude of magnetically-constrained micro-cracks (Levin & Lyutikov 2012). The total strain has two parts,

$$s = s_{\text{el}} + s_{\text{pl}}, \quad (5)$$

where  $s_{\text{el}}$  is given by Equation (4) and  $s_{\text{pl}}$  is the plastic part of the strain. We will use the Bingham-Norton model of an elastic perfectly viscoplastic solid (see e.g. Irgens 2008). It gives the plastic flow rate in the form,

$$\dot{s}_{\text{pl}} = -\frac{\sigma - \sigma_{\text{cr}}}{\eta} \Theta(\sigma - \sigma_{\text{cr}}), \quad (6)$$

where  $\sigma > 0$  is assumed,  $\Theta(X)$  is the Heaviside function, and  $\eta$  is the effective dynamic viscosity. The behaviour of  $\sigma_{\text{cr}}$  has been studied in detail for terrestrial alloys. Two features are common:

(1) Strain hardening:  $\sigma_{\text{cr}}$  may increase with  $|s_{\text{pl}}|$  due to the trapping of dislocations at the boundaries between the alloy grains. On the other hand, recrystallization can occur — the nucleation of new domains that introduce new dislocations. Both effects are neglected below. (2) Thermal softening:  $\sigma_{\text{cr}}$  decreases with temperature, due to the increased mobility of dislocations. In terrestrial alloys, this leads to the formation of shear bands — narrow bands with high  $\dot{s}_{\text{pl}}$ . In a magnetically stressed neutron-star crust thermal softening leads to a TPW. We model the thermal softening in the linear approximation,

$$\sigma_{\text{cr}} = \sigma_0 - \zeta(U_{\text{th}} - U_0), \quad (7)$$

where  $U_{\text{th}}$  is the thermal energy density of a current state,  $U_0$  and  $\sigma_0$  are the thermal energy density and critical stress of some initial state, and  $\zeta$  is a positive constant. Its value may be estimated as follows. At melting temperature  $T_m \sim 3 \times 10^9 \rho_{12}^{1/3}$  K one expects the transition to fluid behavior,  $\sigma_{\text{cr}} = 0$ . The corresponding thermal energy density is  $U_{\text{melt}} \sim \sigma_0/\zeta$ . The ratio of Coulomb lattice energy  $U_{\text{Coul}}$  to its thermal energy at the melting point  $U_{\text{melt}}$  is  $\Gamma \gtrsim 10^2$ . This gives an order-of-magnitude estimate for  $\zeta$ ,

$$\zeta \sim \frac{\sigma_0}{U_{\text{melt}}} \sim \frac{\sigma_0 \Gamma}{U_{\text{Coul}}} \sim \Gamma s_0 \frac{\mu}{U_{\text{Coul}}}. \quad (8)$$

Here  $s_0 = |s|_{\text{max}}$  is the maximum elastic strain of the cold crust at which it must yield, so  $\sigma_0 = \mu s_0$ . At low  $T_0$ , in the absence of mobile dislocations, one would expect  $s_0 \sim 0.1$ , comparable to the yielding threshold for an ideal crystal (Chugunov & Horowitz 2010). Using  $\mu/U_{\text{Coul}} \sim 0.1$  (e.g. Chamel & Haensel 2008), one finds  $\zeta \gtrsim 1$ . Equation (7) can be replaced by more realistic models of thermal softening (Chugunov & Horowitz 2010). The true  $\zeta$  is a function of temperature  $T$ ; it is sensitive to the behavior of heat capacity  $c_V(T)$  and depends on neutron superfluidity.

In contrast to an elastic response, the plastic flow is an irreversible dissipative process. It is accompanied by the heating rate per unit volume  $\dot{q} = -\sigma \dot{s}_{\text{pl}}$ . Heating happens only where the plastic flow occurs, and this can lead to a strong temperature gradient  $\partial T/\partial z$  and significant heat conduction. The thermal equation for the crustal

material then reads

$$\frac{\partial U_{\text{th}}}{\partial t} = -\sigma \dot{s}_{\text{pl}} + \chi \frac{\partial^2 U_{\text{th}}}{\partial z^2}, \quad (9)$$

where  $\chi \approx \kappa/c_V$  the heat diffusion coefficient. Here the simplest model assumes  $\chi = \text{const}$ ; using the estimates of thermal conductivity  $\kappa$  and heat capacity  $c_V$  (e.g. Gnedin et al. 2001), one finds the characteristic  $\chi \sim 10 \text{ cm}^2 \text{ s}^{-1}$  in the deep crust. Equation (9) neglects neutrino cooling; it is assumed to be small compared with plastic heating and heat conduction on the timescales of interest.

The crust is an excellent conductor, and we consider its dynamics on timescales much shorter than the timescale for ohmic dissipation. The field is therefore advected by horizontal displacement of the crust so that

$$\dot{b} = \dot{s}, \quad (10)$$

$$b = s - s_0 + b_0, \quad (11)$$

where  $b_0$  and  $s_0$  are the values of  $b$  and  $s$  at the onset of plastic flow.

Equations (4)-(7), (9), and (11) specify the plastic flow dynamics.

### 3. LOCAL CONVERSION OF MAGNETIC ENERGY TO HEAT

Suppose  $B_y$  is quickly dissipated above the crust, leaving no residual external stress. Then  $b_{\text{ext}} \approx 0$  and Equation (2) gives

$$\sigma = b\mu_B. \quad (12)$$

The density of “free” energy (elastic + magnetic) is given by

$$U_{\text{el}} + U_{\text{mag}} = \frac{\mu s_{\text{el}}^2}{2} + \frac{\mu_B b^2}{2}, \quad (13)$$

and the stress balance (12) implies

$$\frac{U_{\text{el}}}{U_{\text{mag}}} = -\frac{s_{\text{el}}}{b} = \frac{\mu_B}{\mu}. \quad (14)$$

Using Equation (12),  $s_{\text{pl}} = s + \sigma/\mu$ , and  $ds = db$ , one obtains the following expression for the heat generated by the plastic flow:

$$dq = -\sigma ds_{\text{pl}} = -d \left[ \mu_B \frac{b^2}{2} \left( 1 + \frac{\mu_B}{\mu} \right) \right]. \quad (15)$$

It expresses energy conservation:  $dq = -dU_{\text{mag}} - dU_{\text{el}}$ .

For example, consider a magnetar with  $B_z = 4 \times 10^{14}$  G, which corresponds to  $\mu_B = B_z^2/4\pi \approx 10^{28} \text{ erg cm}^{-3}$ . In the deep crust, the shear modulus  $\mu \sim 10^{28} \rho_{12}^{4/3} \text{ erg cm}^{-3}$  exceeds  $\mu_B$ . In this case, in a magneto-elastic equilibrium the stored elastic energy is negligible compared to the energy stored in  $B_y$ :  $U_{\text{mag}} \gg U_{\text{el}}$  and  $|b/s_{\text{el}}| \gg 1$ ; hence  $|s_{\text{el}}| \ll |s_{\text{pl}}|$  and  $s_{\text{pl}} \approx s$ .

It is useful to first consider the plastic flow neglecting heat conduction; this approximation will be relaxed in Section 4. Then the plastically generated heat remains stored locally in the crust,  $dU_{\text{th}} = dq$ , and

$$U_{\text{th}} - U_0 = \mu_B \frac{b_0^2 - b^2}{2} \quad (\chi = 0, \mu \gg \mu_B). \quad (16)$$

For definiteness, we assume  $b > 0$ ; then  $s < 0$  and  $\sigma > 0$ . Equations (6), (7), and (16) give

$$-\eta \dot{s}_{\text{pl}} = \sigma - \sigma_{\text{cr}} = b\mu_B - \sigma_0 + \zeta \mu_B \frac{b_0^2 - b^2}{2}. \quad (17)$$

The plastic flow starts (and stops) at  $\sigma = \sigma_{\text{cr}}$ ;  $\sigma > \sigma_{\text{cr}}$  during the flow. The flow is initiated at  $b = b_0$  and shears the crust so that  $b$  is reduced.

It is instructive to rewrite Equation (17) in the following form,

$$\eta \dot{b} = \frac{\zeta \mu_B}{2} (b - b_0)(b - b_1), \quad (18)$$

where we used  $\dot{s}_{\text{pl}} \approx \dot{s} = \dot{b}$  and

$$b_0 = \frac{\sigma_0}{\mu_B}, \quad b_1 = \frac{2}{\zeta} - b_0. \quad (19)$$

Two conclusions can be drawn from Equations (17) and (18):

(1)  $d\sigma_{\text{cr}}/db > 0$  due to heating with decreasing  $b$ , and a quick plastic relaxation of the magnetic stress is triggered at  $b_0$  if  $d\sigma_{\text{cr}}/db > d\sigma/db = \mu_B$ . Then a plastic deformation reducing  $b$  results in  $\sigma > \sigma_{\text{cr}}$ , which continues to drive  $b$  away from  $b_0$  with an increasing rate; this rate is controlled by viscosity  $\eta$ :  $\dot{b} \approx -(\sigma - \sigma_{\text{cr}})/\eta$ . The condition for this instability,  $d\sigma_{\text{cr}}/db > \mu_B$ , can be re-written as

$$\frac{d\sigma_{\text{cr}}}{dU_{\text{th}}} \frac{dq}{db} > \mu_B. \quad (20)$$

In our simple model with the linear  $\sigma_{\text{cr}}(U_{\text{th}})$  this condition becomes  $\zeta b_0 > 1$ , which is equivalent to  $b_1 < b_0$ . If this condition is not satisfied, the stress relaxation through the thermoplastic instability does not occur; instead there is a slow creep with  $\sigma = \sigma_{\text{cr}}$ . The magneto-elastic balance at the onset of instability gives  $b_0 = (\mu/\mu_B)s_0$  (Equation 14). One can see that  $b_0 \gg s_0$  as long as  $\mu \gg \mu_B$ , and hence the condition  $\zeta b_0 > 1$  can be easily satisfied in the deep crust.

(2) Two final states are possible for the unstable plastic flow. If  $b_1 > 0$ , the flow stops when  $b$  is reduced to  $b_1$ ; then it freezes with  $\sigma > 0$ . The total energy density dissipated by the plastic flow is then given by

$$q = \frac{\mu_B}{2} (b_0^2 - b_1^2), \quad (b_1 > 0). \quad (21)$$

If  $b_1 < 0$ ,  $\sigma_{\text{cr}}$  vanishes at some  $b_{\text{melt}}$  ( $0 < b_{\text{melt}} < b_0$ ). In this case, the crust melts during the plastic flow and becomes fluid, with negligible elastic stress; the magnetic field will then relax to the stress-free state with  $b \approx 0$ . Then all free energy is converted to heat,  $q \approx \mu_B b_0^2/2$ .

The temperature achievable by converting magnetic energy to heat is  $T \sim B_y^2/8\pi c_V$ . Using the heat capacity  $c_V \sim 10^{18} - 10^{19}$  erg cm<sup>-3</sup> K<sup>-1</sup> (its exact value depends on neutron superfluidity, Gnedin et al. 2001), one finds  $T \sim 10^9 - 10^{10} B_{y,15}^2$  K. It may exceed the melting temperature.

The characteristic timescale of the unstable flow may be estimated from Equation (18). Besides time  $t$ , it contains only two quantities of non-zero dimension,  $\mu_B$  and  $\eta$ . Their ratio defines the timescale for the local energy release,

$$\Delta t \sim \frac{\eta}{\mu_B}. \quad (22)$$

#### 4. THERMOPLASTIC WAVE

A TPW is analogous to a deflagration front. Both phenomena operate on two essential ingredients: (1) Local heating/burning rate increases with temperature. For deflagration this is a chemical reaction while for TPW this is the temperature-sensitive plastic flow. (2) Heat conduction helps the burning to spread. In our case, the horizontal magnetic field plays the role of unburned fuel; it is “consumed” by the induced plastic flow.

Consider a crust that is stressed by a slowly evolving magnetic field so that  $\sigma$  gradually approaches the critical value  $\sigma_{\text{cr}}$ . It first reaches  $\sigma_{\text{cr}}$  at some  $z_0$ . The plastic flow initiated at  $z_0$  generates heat, which is conducted to the neighborhood of  $z_0$  where  $\sigma(z)$  is initially smaller than  $\sigma_{\text{cr}}(z)$ . The spreading heat reduces  $\sigma_{\text{cr}}$  and can lead to  $\sigma_{\text{cr}} < \sigma$  so that the region of plastic flow can spread upward and downward. When the characteristic thickness of the heated layer reaches  $l$  estimated below, heat conduction is marginally able to cool it. Then the thermoplastic instability launches a wave resembling the deflagration front in combustion physics.

The propagation speed of the TPW is determined by the heat diffusion coefficient  $\chi$  and viscosity  $\eta$ . Recall that  $\eta$  sets the characteristic timescale of “burning” the magnetic energy density  $\Delta t$  (Equation 22) while the characteristic width of the burning front  $l$  is related to  $\chi$  by

$$l \sim (\chi \Delta t)^{1/2}. \quad (23)$$

The front velocity is

$$v \sim \frac{l}{\Delta t} \sim \left( \frac{\chi \mu_B}{\eta} \right)^{1/2}. \quad (24)$$

The parameters of the crust ahead of the front vary with  $z$  on the hydrostatic scale  $H$ . The heating front with the characteristic thickness  $l \ll H$  is a quasi-steady propagating structure where all parameters are functions of  $u = z - vt$ . The front structure is described by the plastic stress Equation (6) and the thermal Equation (9). Using  $\partial/\partial t = -v d/du$  and  $\partial/\partial z = d/du$ , these equations give

$$v\eta \frac{db}{du} = \mu_B(b - b_0) + \zeta(U_{\text{th}} - U_0), \quad (25)$$

$$\chi \frac{dU_{\text{th}}}{du} = -v \left[ \frac{\mu_B}{2} (b^2 - b_0^2) + U_{\text{th}} \right], \quad (26)$$

where we used Equation (15) for the generated plastic heat. We choose  $u = 0$  where the flow is initiated;  $\sigma = \sigma_{\text{cr}}(U_0)$  at this point. Far ahead of the front the crust is cold ( $U_{\text{th}} \approx 0$ ) and stable,  $\sigma < \sigma_{\text{cr}}(0)$ . The ratio  $f = \sigma_{\text{cr}}(0)/\sigma_{\text{cr}}(U_0) > 1$  determines how much preheating (through heat conduction) occurs ahead of plastic flow zone.

Equations (25) and (26) can be solved as follows. We divide them and obtain one equation for  $w = U_{\text{th}}/\mu_B$  as a function of  $b$ ,

$$\frac{dw}{db} = -p \frac{[w - (b_0^2 - b^2)/2]}{\zeta w - b_0 f + b}, \quad p \equiv \frac{v^2 \eta}{\chi \mu_B}. \quad (27)$$

This equation has a critical point where the numerator and denominator must vanish simultaneously. As long

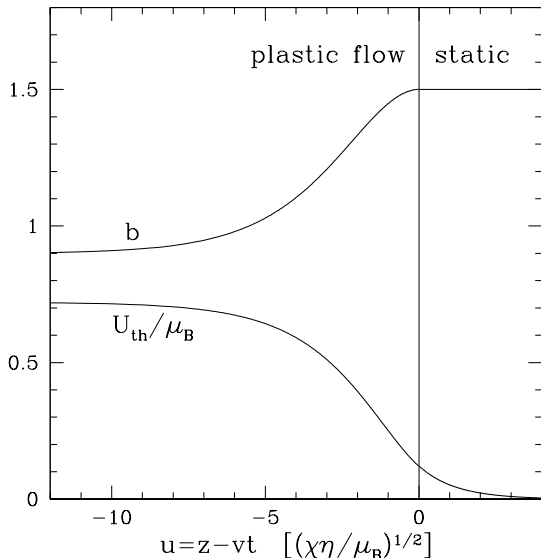


FIG. 1.— TPW structure calculated for  $\zeta = 1$ ,  $b_0 = 1.5$ , and  $f = 1.08$ . In this case, we find  $p = 0.714$ .

as  $2f < \zeta b_0 + (\zeta b_0)^{-1}$ , this point is reached at

$$b_1 = \frac{1}{\zeta} \left[ 1 - \sqrt{(\zeta b_0 - 1)^2 - 2\zeta b_0(f - 1)} \right]. \quad (28)$$

We will assume  $b_1 > 0$ . Note that  $db/du \rightarrow 0$  and  $dU_{th}/du \rightarrow 0$  as  $b$  approaches  $b_1$ , and hence  $b_1$  represents the asymptotic downstream state of the crust behind the front.

For any given parameter  $p$  Equation (27) can be integrated from  $b = b_0$  towards smaller  $b$ , which gives a solution  $w(b)$ . Only one value of  $p$  gives  $w(b)$  that satisfies the regularity condition at  $b_1$ . We find the required  $p$  and the corresponding solution  $w(b)$  numerically, using iterations. This determines the front velocity  $v = (p\chi\mu_B/\eta)^{1/2}$ . Then, using the known  $v$  and the obtained relation between  $b$  and  $w$  we integrate Equations (25) and (26). A sample solution is shown in Figure 3. The model assumes constant diffusion coefficients  $\eta$  and  $\chi$ ; extension to models with temperature-dependent  $\eta$  and  $\chi$  is straightforward.

## 5. TWISTING THE EXTERNAL MAGNETIC FIELD

Consider now an axisymmetric crustal plate in a cylindrical coordinate system  $(r, \phi, z)$ . If gradients along  $z$  are much greater than gradients along  $r$  (the depth of the crustal plate much smaller than its radius) our plate is locally approximated by the slab model described in Sections 2-4 with  $x = r$ ,  $y = r\phi$ , and  $B_y = B_\phi$ . Dissipation of toroidal field  $B_\phi$  by the thermoplastic front propagating vertically inside the plate causes its rotation in the  $\phi$  direction (Figure 2).

Once the pair of upward and downward fronts are launched from the plastically heated region, the upper crust starts to rotate with respect to the static lower crust. Each crustal layer crossed by the front is sheared by  $\Delta s = b_1 - b_0$ , and propagation of the two fronts in time  $dt$  rotates the upper crust by  $d\xi = -2(b_0 - b_1)vdt$ .

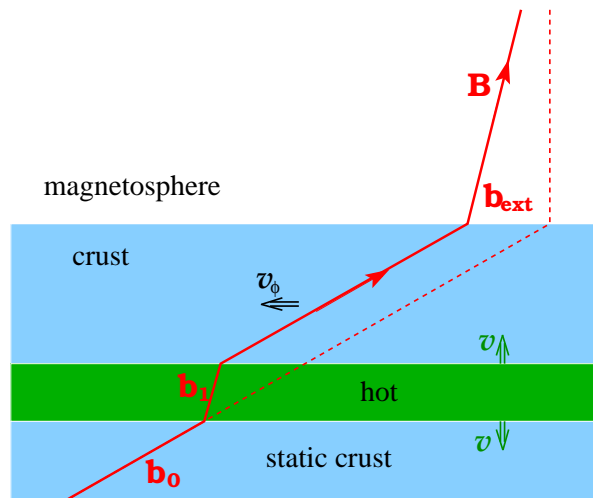


FIG. 2.— The crustal plate above the plastically heated layer moves with horizontal velocity  $v_\phi$  that is related to the TPW velocity  $v$  by the kinematic constraint  $v_\phi = -2(b_0 - b_1)v$ . Magnetic field lines are shown in red; they are frozen in the crustal material;  $b = B_\phi/B_z$ . Dotted line shows the magnetic field line before the pair of TPW was launched.

This gives the rotation velocity of the plate,

$$v_\phi = \frac{d\xi}{dt} = -2(b_0 - b_1)v, \quad (29)$$

which twists the external magnetosphere attached to it. The magnetosphere is force-free, i.e. electric current  $\mathbf{j}$  associated with  $B_\phi$  must flow along  $\mathbf{B}$ . The magnetospheric current penetrates the plate only where rotation is differential in the horizontal plane,  $d/dr(v_\phi/r) \neq 0$ ; in the region of rigid rotation the circuit closes horizontally along the plate surface (Beloborodov 2009).

Consider a dipole magnetosphere and let our plate be a polar cap (or a ring) of radius  $r_0 = R \sin \theta_0$ , where  $R$  is the star radius. The field component normal to the surface,  $B_R$ , plays the role of  $B_z$  in previous sections, so  $\mu_B = B_R^2/4\pi$ . The plate displacement  $d\xi$  twists the external magnetic field lines by angle  $d\psi \approx -d\xi/r_0$  (assuming their footprints in the other hemisphere are static). An external stress  $\mu_B b_{\text{ext}}$  is then generated above the plate, where  $b = B_\phi/B_R$ . Using the relation between  $B_\phi$  and  $\psi$  for a moderately twisted dipole magnetosphere (Beloborodov 2009), we find  $b_{\text{ext}} \approx (\psi/4)(\sin^3 \theta_0 / \cos^2 \theta_0)$ .

The rotating plate pumps  $b_{\text{ext}}$  with rate  $\dot{b}_{\text{ext}} \propto \dot{\psi} \propto -v_\phi$ . On the other hand, the external twist is damped on the ohmic timescale  $t_{\text{ohm}}$ , because sustaining magnetospheric currents requires voltage  $\Phi \sim 10^9 - 10^{10}$  V (Beloborodov & Thompson 2007). The resulting evolution equation for  $b_{\text{ext}}$  reads

$$\frac{db_{\text{ext}}}{dt} = \frac{\dot{\psi} \sin^3 \theta_0}{4 \cos^2 \theta_0}, \quad \dot{\psi} = \frac{2b_0 v}{r_0} - \dot{\psi}_{\text{ohm}}. \quad (30)$$

A detailed derivation of the ohmic damping  $\dot{\psi}_{\text{ohm}} \sim 1 \text{ rad yr}^{-1}$  is given in Beloborodov (2011). Delivering the external twist  $\dot{\psi} > 0$  requires a sufficiently fast propagation of the thermoplastic front,  $v \gtrsim \dot{\psi}_{\text{ohm}} r_0 / 2b_0 \sim 10^{-3} r_{0,\text{km}} / b_0 \text{ cm s}^{-1}$ . Comparing with Equation (24), we find that this condition translates to an upper bound

on the (unknown) viscosity of the plastic flow,  $\eta < \chi B_\phi^2 / \pi \psi_{\text{ohm}}^2 r_0^2 \sim 10^{35}$  erg s cm $^{-3}$ .

If the rotating plate is near the magnetic pole,  $\theta_0 < 1$ , even a strong twist  $\psi \sim 1$  corresponds to a small  $b_{\text{ext}} \ll 1$ . In this case, neglecting  $b_{\text{ext}}$  in the TPW model is a valid assumption. Significant  $b_{\text{ext}}$  can be generated at large  $\theta_0$ . Equation (2) shows how this would reduce the elastic stress inside the plate,

$$\sigma = \mu_B(b - b_{\text{ext}}). \quad (31)$$

When  $b_{\text{ext}}$  becomes comparable to  $b$ , the TPW will be choked. Later  $b_{\text{ext}}$  is damped ohmically in the magnetosphere,  $\sigma$  rises and the front can be launched again.

The heating rate in the front is  $\dot{q} \sim B_\phi^2 / 8\pi \Delta t$ , where  $\Delta t$  is related to the front velocity  $v$  by  $\Delta t \sim \chi / v^2$ . This gives

$$\dot{q} \sim \frac{B_\phi^2 v^2}{8\pi \chi}. \quad (32)$$

The condition  $v > v_{\text{min}} \sim \dot{\psi}_{\text{ohm}} r_0 / 2b_0$  corresponds to a minimum heating rate

$$\dot{q}_{\text{min}} \sim 10^{-2} \frac{B_R^2 r_0^2 \psi_{\text{ohm}}^2}{\chi}. \quad (33)$$

Using  $B_R \sim 3 \times 10^{14}$  G typical for magnetars,  $\dot{\psi}_{\text{ohm}} \sim 1$  rad yr $^{-1}$ , and  $\chi \sim 10$  cm $^2$  s $^{-1}$ , we estimate  $\dot{q}_{\text{min}} \sim 10^{22}$  erg cm $^{-3}$  s $^{-1}$ . The minimum heating exceeds neutrino cooling  $\dot{q}_\nu \sim 10^{21}$  erg cm $^{-3}$  s $^{-1}$  (e.g. Gnedin et al. 2001), which vindicates our neglect of neutrino cooling in the TPW model. Heating is concentrated in the thin front,  $l < \chi / v_{\text{min}} \sim 100$  m, and neutrino emission cools the heated crust *behind* the front before it propagates a distance comparable to the crust thickness.

Creating the external twist by the TPW is inevitably accompanied by dissipation at large depths where heat is drained by neutrino emission (Kaminker et al. 2009). It is useful to compare the energy flux delivered into the external twist  $F_{\text{tw}} = -v_\phi b_{\text{ext}} \mu_B$  with the internal dissipation rate per unit area,  $F_{\text{diss}} \approx v(b_0^2 - b_1^2) \mu_B$ ,

$$\frac{F_{\text{tw}}}{F_{\text{diss}}} = \frac{2b_{\text{ext}}}{b_0 + b_1} \approx \frac{\psi \sin^3 \theta_0}{2(b_0 + b_1) \cos^2 \theta_0}. \quad (34)$$

## 6. DISCUSSION

The proposed mode of rapid plastic motion exists only in materials that are magnetically stressed to breaking point; it remains to be seen whether it could be produced in a high-B terrestrial experiment. TPW is likely to operate in magnetars and shape their observed activity by rapidly dissipating magnetic energy inside the crust and by twisting the external magnetosphere.

The thermoplastic front heats the crust so strongly that it may melt it and destroy neutron superfluidity. The melted material crystalizes behind the front on the neutrino cooling timescale. The lifting of superfluidity can transfer angular momentum from neutron superfluid to the lattice and produce a spin-up "glitch."

A TPW at low magnetic latitudes is choked when the external  $B_\phi$  becomes comparable to the internal  $B_\phi$ , and is revived after the external twist has been ohmically damped. Repeated crustal shearing is generally expected, leading to repeating events of magnetar activity. The duration of these events is controlled by the speed of the TPW, which determines the shear rate of the crust. This rate cannot be smaller than  $\sim 1$  rad s $^{-1}$  and is likely much higher. However, it is not high enough to explain the duration of magnetar bursts  $\sim 0.1 - 0.3$  s. The bursts must be triggered in the magnetosphere, like solar flares, or by a faster failure mode of the crust that is yet to be identified. The burst duration is likely set by the mechanism of energy dissipation taking significantly longer than the Alfvén crossing time of the magnetosphere.

Our description of a TPW delivering external twists works for a broad range of viscosity  $\eta \lesssim 10^{35}$  erg s cm $^{-3}$ . A weak lower bound  $\eta > 10^{12}$  erg s cm $^{-3}$  is provided by electron viscosity (Chugunov & Yakovlev 2005). A more relevant estimate may come from phonon viscosity, as the phonon gas exerts drag on the thermally activated dislocations (Mason 1960).

Our future work will extend the TPW model to explicitly include the build up of magnetic stresses due to Hall drift. Multidimensional simulations could show the beginning and development of the TPW into the propagating front described in this Letter. Future models will invoke the global crust structure with accurate heat capacity and thermal conductivity.

AMB acknowledges support by NASA grant NNX13AI34G. YL's research was supported by the Monash Research Acceleration grant. We thank Andrei Chugunov for discussions, and Sarah Levin for help with the prose.

## REFERENCES

- An, H., Hascoët, R., Kaspi, V. M., et al. 2013, ApJ, 779, 163  
 Beloborodov, A. M. 2009, ApJ, 703, 1044  
 Beloborodov, A. M. 2011a, in High-Energy Emission from Pulsars and their Systems, Astrophysics and Space Science Proceedings, ed. D. F. Torres & N. Rea (Berlin: Springer), 299  
 Beloborodov, A. M. 2013, ApJ, 762, 13  
 Beloborodov, A. M., & Thompson, C. 2007, ApJ, 657, 967  
 Chamel, N., & Haensel, P. 2008, LRR, 11, 10  
 Chugunov, A. I., & Horowitz, C. J. 2010, MNRAS, 407, L54  
 Chugunov A. I., & Yakovlev D. G., 2005, Astron. Rep., 49, 724  
 Gnedin, O. Y., Yakovlev, D. G., & Potekhin, A. Y. 2001, MNRAS, 324, 725  
 Goldreich, P., & Reisenegger, A. 1992, ApJ, 395, 250  
 Gotthelf, E. V., & Halpern, J. P. 2007, Ap&SS, 308, 79  
 Hascoët, R., Beloborodov, A. M., & den Hartog, P. R. 2014, ApJ, 786, L1  
 Irgens, F. 2008, Continuum Mechanics, Berlin: Springer-Verlag  
 Jones, P. B. 2003, ApJ, 595, 342  
 Kaminker, A. D., Potekhin, A. Y., Yakovlev, D. G., & Chabrier, G. 2009, MNRAS, 395, 2257  
 Kobayakov, D., & Pethick, C. J. 2014, Phys. Rev. Lett., 112, id.112504  
 Levin, Y., & Lyutikov, M. 2012, MNRAS, 427, 1574L  
 Lyutikov, M. 2006, MNRAS, 367, 1594  
 Mason, W. P. 1960, J. Acoust. Soc. Am. 32, 458  
 Mereghetti, S. 2008, A&ARv, 15, 225  
 Parfrey, K., Beloborodov, A. M., & Hui, L. 2013, ApJ, 774, 92  
 Thompson, C., & Duncan, R. C. 1996, ApJ, 473, 322  
 Thompson, C., Lyutikov, M., & Kulkarni, S. R. 2002, ApJ, 574, 332  
 Viganò, D., Rea, N., Pons, J. A., et al. 2013, MNRAS, 434, 123